11th World Congress on Computational Mechanics (WCCM XI)
5th European Conference on Computational Mechanics (ECCM V)
6th European Conference on Computational Fluid Dynamics (ECFD VI)
E. Oñate, J. Oliver and A. Huerta (Eds)

HOMOGENIZED GLOBAL NONLINEAR CONSTITUTIVE MODEL FOR RC PANELS UNDER CYCLIC LOADINGS

MIQUEL HUGUET[*†], FRANÇOIS VOLDOIRE[§], PANAGIOTIS KOTRONIS[*] AND SILVANO ERLICHER[†],

[*] LUNAM Université, Ecole Centrale de Nantes, Université de Nantes, CNRS
Institut de Recherche en Génie Civil et Mécanique (GeM)
1 rue de la Nöe 44321 Nantes, France
e-mail: panagiotis.kotronis@ec-nantes.fr, www.ec-nantes.fr

[†] EGIS Industries
4 Dolorès Ibarruri 93188 Montreuil, France
email: miquel.huguet-aguilera@egis.fr, silvano.erlicher@egis.fr, www.egis.fr

[§] Electricité de France R&D/AMA
Laboratoire de Mécanique des Structures Industrielles Durables, UMR EDF–CNRS–CEA 8193
1 Avenue du Général de Gaulle F-92141, Clamart, France
email: francois.voldoire@edf.fr, www.edf.fr

Key Words: *Nonlinear analysis, Seismic design, Cracking, Global model, RC panels*

Summary. *A new nonlinear stress resultant global constitutive model for RC panels is presented. Concrete damage, concrete stress transfer at cracks and bond-slip stress are the main nonlinear effects identified at the local scale that constitute the basis for the construction of the stress resultant global model through an analytical homogenization technique. The closed form solution is obtained using general functions for the previous phenomena.*

1 INTRODUCTION

Industrial buildings, in particular Nuclear Power Plants (NPP), are subjected to severe seismic requirements. These facilities, generally built in Reinforced Concrete (RC), have large dimensions and therefore time-expensive dynamic analyses are necessary. The use of global modeling approaches, which relate the stress resultant $\boldsymbol{\sigma}^o$ with the generalized strains $\boldsymbol{\varepsilon}^o$ using relative big size finite elements of RC material, can assure reasonable computational costs, numerical efficiency and robustness. This type of modeling strategy is often used in civil engineering design offices adopting linear elastic constitutive laws. However, recent requirements for NPP have led to the use of more realistic RC non-linear models.

In this sense, two global nonlinear constitutive models for RC shells have been recently introduced in the Finite Element (FE) software *Code_Aster* [1], commonly used for the static and dynamic (including seismic) analysis of industrial buildings in France and, more specifically, for NPP. Initially, the GLRC_DM model [2] based on global damage variables describing the mechanical non-linearities in the entire Serviceability Limit State (SLS) domain (for moderate seismicity regions) was developed, but it was soon observed that this approach underestimates the energy dissipation for the case of cyclic loadings, even though the stiffness reduction effect in RC building natural frequencies is quite well reproduced. The performance was significantly improved considering the debonding between steel and concrete through a numerical homogenization procedure, developed in the DHRC model [3]. Both models are formulated according to the General Standard Materials Theory (GSMT) [4] within the framework of the Thermodynamics of Irreversible Processes (TIP) [5], allowing a well-defined energetic characterization and adapted for a time integration algorithm associated with a well-posed minimization problem. These choices ensure a high degree of robustness and versatility to any dynamic loading conditions that can occur at a RC building FE analysis.

However, the previous global modeling approaches do not take explicitly into account phenomena of great importance for industrial facilities, (especially for confinement issues in NPP) such as crack apparition and evolution. The crack parameters (orientation, spacing and width) are thus often computed adopting suitable post-processing techniques. The limitations of this two-step procedure for the computation of the crack parameters as a post-processing of a FE analysis have been highlighted in [6], where the *phenomenological* constitutive model for cracked panels called Cracked Membrane Model (CMM) [7] has been used.

Other *phenomenological* models are available in the literature, see for example [8]-[9]. In these approaches, cracking in RC panels is described by adopting suitable hypotheses or specific laws for the local scale physical phenomena that govern the nonlinear structural response. In general, they are only applicable to particular loadings (e.g. only for monotonic loadings) or states (e.g. only for a fully cracked panel) since they are developed and calibrated based on particular experimental campaigns (some exceptions exists, see the cyclic *phenomenological* model [10]). Furthermore, their numerical algorithms require iterations to fulfill the conditions at the local scale phenomena because the link between the local and global scales is not explicitly described. Therefore, their robust implementation at the global scale in a FE software is not straightforward.

In this work, a novel global constitutive model for RC walls is presented taking into account three sources of non-linearities at the local scale: (i) concrete damage or micro-cracking, which causes a reduction in the concrete stiffness through a damage variable, (ii) concrete macro-cracking with non-zero stresses at cracks and (iii) bond stresses caused by the relative displacement between concrete and steel bars. We describe the successive assumptions adopted in the model formulation. The obtained stress resultant $\boldsymbol{\sigma}^O$ - $\boldsymbol{\varepsilon}^O$ generalized strains relationship takes into account the previous nonlinear phenomena as long as it is obtained by means of an analytical homogenization procedure where they explicitly appear.

2 GEOMETRY OF THE RC PANEL

Let us consider a RC panel of dimensions L_x, L_y and width h submitted to in-plane loads (Figure 1). Flexural effects are not considered and consequently all the reinforcement grids can be merged at the mid-plane. The x and y axes define the direction of the two groups of the steel bars, characterized by their diameters ϕ_x and ϕ_y and their spacings e_x and e_y, respectively. The three components of the RC panel are identified with the following indexes: c for concrete, and sx and sy for the steel bars in the x and y directions respectively.

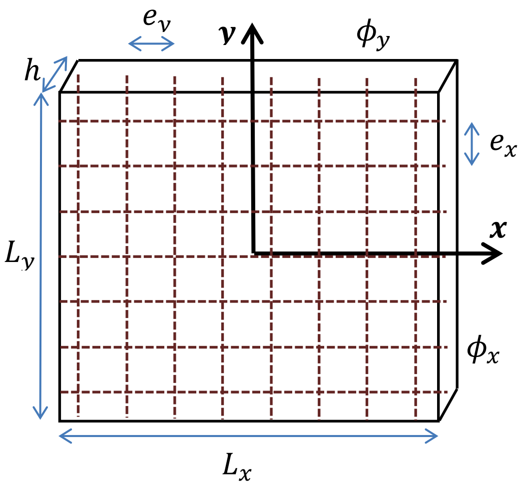

Figure 1: Geometry of the RC panel

3 MATERIAL MODELING

The steel reinforcement bars are supposed to be a one-dimensional medium and to carry only longitudinal forces. Therefore, they are modeled using a one-dimensional linear elastic constitutive law (since the interest domain of the present model is the SLS), with $E_{s\alpha}$ the Young modulus and $\otimes$ the dyadic tensor product):

$$\boldsymbol{\sigma}^{s\alpha} = E_{s\alpha}\, \varepsilon_{\alpha\alpha}^{s\alpha} \cdot \underline{e}_\alpha \otimes \underline{e}_\alpha \qquad \alpha = x, y \tag{1}$$

The global nonlinear response of the model has its origin at the three nonlinear phenomena at the local scale: concrete damage, apparition of macro-cracking (and development of stress transfer by concrete at cracks) and bond stress between concrete and steel rebars.

Concrete damage, caused by the apparition and development of rather homogeneous diffuse micro-cracking, results in concrete stiffness reduction, introduced via an internal damage scalar variable d, directly affecting the concrete Young Modulus E_c. The relationship between the membrane stresses and strains (plane stress state, local concrete isotropic constitutive law) is expressed as follows:

$$\begin{pmatrix} \sigma_{xx}^c \\ \sigma_{yy}^c \\ \sigma_{xy}^c \end{pmatrix} = \frac{E_c(d)}{1-\nu_c^2} \begin{pmatrix} 1 & \nu_c & 0 \\ \nu_c & 1 & 0 \\ 0 & 0 & 1-\nu_c \end{pmatrix} \cdot \begin{pmatrix} \varepsilon_{xx}^c \\ \varepsilon_{yy}^c \\ \varepsilon_{xy}^c \end{pmatrix} \tag{2}$$

Concrete cracking (apparition of macro-cracks) is seen as localized concrete displacement discontinuities $\underline{w} = (w_n, w_t)$ in the normal-to-crack direction (or crack width) w_n and in the tangential direction w_t. The apparition of a macro-crack occurs when the maximum principal concrete stress σ_1^c reaches the concrete tensile stress f_{ct}. In other words, the adopted macro-cracking criterion is the classical Rankine criterion expressed as:

$$F(\boldsymbol{\sigma}^c) = \sigma_1^c - f_{ct} \leq 0 \tag{3}$$

This criterion separates the behavior of the RC panel in two different phases: the uncracked and the cracked one. The cracked phase can also be divided in two parts: the crack formation (some cracks exist but other appear with increasing loading) and the stabilized crack phase (no more cracks appear even with increasing loading), see e.g. [11]. However, the crack formation phase can be considered to be negligible in a finite element with the usual modeling dimensions, and in this work only the uncracked and the stabilized cracked phases are considered. At cracks, the concrete stress transfer vector $\underline{g}$ is considered, which has a normal and a tangential component named g_n and g_t respectively. They both depend on the crack opening displacement field $\underline{w}$ and other internal variables noted hereafter $\underline{v}_g$:

$$\underline{g} = \underline{g}\left(w_n, w_t, \underline{v}_g\right) \tag{4}$$

Finally, bond stresses $\underline{\tau}_d = \left(\tau_x, \tau_y\right)$ transmitted from x and y reinforcement steel bars to concrete are at the origin of the *tension stiffening* effect. They appear when a relative slip $\underline{s} = \left(s_x, s_y\right)$ or steel-concrete debonding, associated with internal variables $\underline{v}_s$, occurs:

$$\underline{\tau}_d = \underline{\tau}_d\left(s_x, s_y, \underline{v}_s\right) \tag{5}$$

4 ANALYTICAL HOMOGENIZATION OF THE CRACKED RC PANEL

In this section an analytical homogenization of a cracked RC panel is performed. In a region of the panel far enough from non-regular boundary conditions, an identifiable periodicity has to be identified in order to define the Reference Volume Element (RVE) of the problem, that is the smallest volume able to represent the physical phenomena governing the response of the material and which is repeated periodically in the space. After the identification of the RVE, referring for instance to [12], the following steps, represented schematically in Figure 2, have to be done:

i) Definition of the local stress fields $\boldsymbol{\sigma}^c, \boldsymbol{\sigma}^{sx}, \boldsymbol{\sigma}^{sy}$ as functions of an applied stress resultant $\boldsymbol{\sigma}^o$ on the RVE (stress localization).

ii) Application of the local constitutive laws to obtain the local strain fields $\boldsymbol{\varepsilon}^c, \boldsymbol{\varepsilon}^{sx}, \boldsymbol{\varepsilon}^{sy}$.

iii) Application of the compatibility equations and the averaging method to obtain the generalized strain field $\boldsymbol{\varepsilon}^o$ from the previous calculated fields.

$$\begin{tikzcd}
\boldsymbol{\sigma}^o \arrow[rr, leftrightarrow, "\text{Global law}"] \arrow[d, "\text{Localization} + \text{Averaging}"'] & & \boldsymbol{\varepsilon}^o \\
\underset{\boldsymbol{\sigma}^c, \boldsymbol{\sigma}^{sx}, \boldsymbol{\sigma}^{sy}}{\boldsymbol{\sigma}^{loc}} \arrow[rr, "\text{Local constitutive laws}"'] & & \underset{\boldsymbol{\varepsilon}^c, \boldsymbol{\varepsilon}^{sx}, \boldsymbol{\varepsilon}^{sy}}{\boldsymbol{\varepsilon}^{loc}} \arrow[u, "\text{Compatibility} + \text{Averaging}"']
\end{tikzcd}$$

Figure 2: Homogenization technique scheme

Even though it is more usual to formulate this scheme by beginning with the strain field, we prefer to take the stress resultant field to apply directly some useful equilibrium arguments in the formulation. In steps i) and iii) the local-global scales passage is done by means of the averaging method, based on the average value of a considered field in the RVE volume Ω:

$$\langle \cdot \rangle_\Omega = \frac{1}{|\Omega|} \int_\Omega \cdot \, dv \tag{6}$$

4.1 The Representative Volume Element

The panel in the stabilized crack configuration of Figure 3 is considered as a periodic succession of RC ties separated by two consecutive cracks, with orientation $-\frac{\pi}{2} \leq \theta_r \leq \frac{\pi}{2}$ from the x axis and mean spacing s_r. One of these straight ties is chosen as the RVE of the problem, where we define the normal to crack N and tangential T axes as follows:

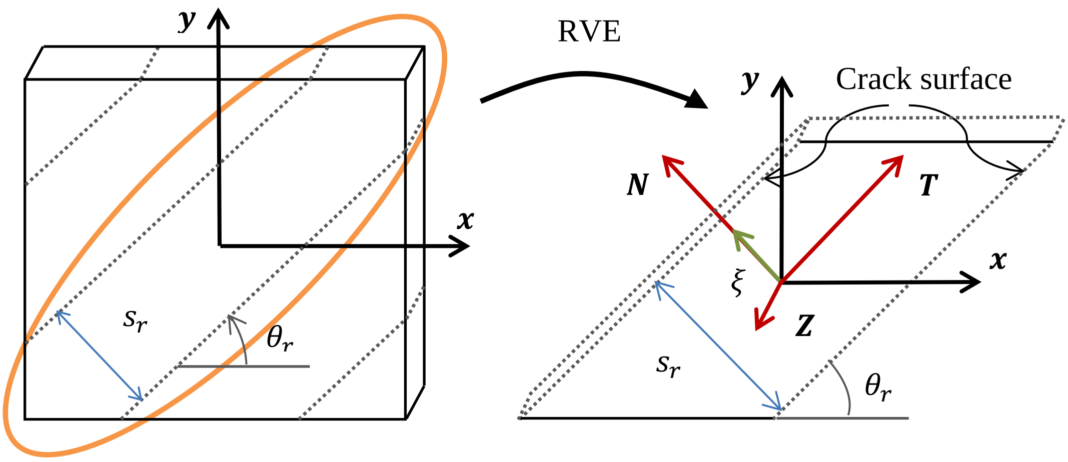

Figure 3: Representative Volume Element of a cracked panel

Within the RVE, we adopt the assumption that all fields are constant in the Z direction (they do not vary within the width h), and in the T direction (since the RVE dimensions in the N direction is the crack spacing $s_r \ll L_x, L_y$ and the boundary conditions at cracks are constant); the fields depend thus only on the ξ dimensionless coordinate. Moreover, $T - Z$ constitutes a symmetry plane. Under these assumptions, the average value (6) of any field in the RVE is calculated according to:

$$\langle \cdot \rangle_\Omega = \langle \cdot \, (\xi) \rangle_\Omega = \frac{1}{2} \int_{-1}^{1} \cdot \, (\xi) d\xi = \int_{0}^{1} \cdot \, (\xi) d\xi \tag{7}$$

The steel bars are considered uniformly distributed in the RVE, since $e_x, e_y \ll L_x, L_y$ and the continuum stress fields $\boldsymbol{\sigma}^i\ (\xi)\ (i = sx, sy, c\ )$ are considered into the entire RVE. Only surface forces are applied at the limit with the bordering RVE and the $\boldsymbol{\sigma}^o$ stresses are transmitted. Under the previous assumptions a constant stress resultant is defined on the RVE:

$$\boldsymbol{\sigma}^o(\xi) = \boldsymbol{\sigma}^o \qquad \forall \xi \tag{8}$$

4.2 Stress resultant localization

The stress resultant localization (see Figure 2) consists in calculating the local stress fields in the RVE when a stress resultant $\boldsymbol{\sigma}^o$ is applied. In the present case, it consists on determining nine unknowns: the three planar components of the three (concrete and x and y steel bars) components local stress fields.

First, we define the concrete and x and y steel bars local stress field averages with the equation (6) :

$$\langle\boldsymbol{\sigma}^i\rangle \equiv \langle\boldsymbol{\sigma}^i\rangle_{\Omega_i} = \frac{1}{|\Omega_i|}\int_{\Omega_i} \boldsymbol{\sigma}^i \, dv \qquad i = c, sx, sy \tag{9}$$

with Ω_i the volume of component i in the RVE ($\Omega_c + \Omega_{sx} + \Omega_{sy} = \Omega$). The stress resultant can be expressed as:

$$\boldsymbol{\sigma}^o = \frac{h}{|\Omega|}\int_{\Omega} \boldsymbol{\sigma} \, dv = h \cdot \left(\rho_c\langle\boldsymbol{\sigma}^c\rangle + \rho_{sx}\langle\boldsymbol{\sigma}^{sx}\rangle + \rho_{sy}\langle\boldsymbol{\sigma}^{sy}\rangle\right) \tag{10}$$

where the volume fractions ρ_i have been used:

$$\rho_i = \frac{|\Omega_i|}{|\Omega|} \qquad i = c, sx, sy \tag{11}$$

In the considered RC panel they can be calculated as:

$$\rho_{sx} = \frac{\pi\phi_x^2}{4he_x} \qquad \rho_{sy} = \frac{\pi\phi_y^2}{4he_y} \qquad \rho_c = 1 - \rho_{sx} - \rho_{sy} \tag{12}$$

Equation (10) can be expressed, in a closed form (true in any point, not only for the stresses averages in the RVE) by using (8):

$$\boldsymbol{\sigma}^o = h \cdot \left(\rho_c\boldsymbol{\sigma}^c(\xi) + \rho_{sx}\boldsymbol{\sigma}^{sx}(\xi) + \rho_{sy}\boldsymbol{\sigma}^{sy}(\xi)\right) \qquad \forall\xi \tag{13}$$

Second, the equilibrium equation for the concrete component in the entire RVE reads:

$$\underline{\nabla} \cdot \boldsymbol{\sigma}^c(\xi) + \underline{b}^c(\xi) = \underline{0} \tag{14}$$

where $\underline{\nabla}$ stands for the divergence operator and $\underline{b}^c(\xi)$ for the volume forces vector (only caused by a diffuse action by bond stress from steel bars on the concrete domain), which can be obtained from the equilibrium in a differential volume:

$$b_\alpha^c = \frac{4\tau_\alpha(\xi)\rho_{s\alpha}}{\phi_\alpha\rho_c} \tag{15}$$

Finally, according to the steel constitutive law (1) the two non-axial components of x and y rebars stress fields vanish. These four equations are added to the three equations from the global-local relationship (13) and the two from the concrete equilibrium (14) to form a nine equations system that determines the local stress fields:

$$\begin{cases} \boldsymbol{\sigma}^o = h \cdot \left(\rho_c\boldsymbol{\sigma}^c(\xi) + \rho_{sx}\boldsymbol{\sigma}^{sx}(\xi) + \rho_{sy}\boldsymbol{\sigma}^{sy}(\xi)\right) \\ \underline{\nabla} \cdot \boldsymbol{\sigma}^c(\xi) + \underline{b}^c(\xi) = \underline{0} \\ \sigma_{xy}^{sx}(\xi) = \sigma_{yy}^{sx}(\xi) = \sigma_{xx}^{sy}(\xi) = \sigma_{xy}^{sy}(\xi) = 0 \end{cases} \tag{16}$$

The two boundary conditions for the two differential equations of the concrete equilibrium stem from the definition of concrete stresses at cracks:

$$\begin{cases} \sigma_{nn}^{c}(\xi = \pm 1) = g_n \\ \sigma_{tn}^{c}(\xi = \pm 1) = g_t \end{cases} \tag{17}$$

The following solution is obtained for the local concrete and steel stress fields $\boldsymbol{\sigma}^{c}$, $\boldsymbol{\sigma}^{sx}$ and $\boldsymbol{\sigma}^{sy}$:

$$\begin{pmatrix} \sigma_{xx}^{c}(\xi) \\ \sigma_{yy}^{c}(\xi) \\ \sigma_{xy}^{c}(\xi) \end{pmatrix} = \begin{pmatrix} \dfrac{\sigma_{xy}^{o}}{\rho_c h \tan\theta_r} - \dfrac{2 s_r \rho_{sx}}{\phi_x \rho_c \sin\theta_r} \displaystyle\int_{|\xi|}^{1} \tau_x(s) ds + g_n - \dfrac{1}{\tan\theta_r} g_t \\ \tan\theta_r \dfrac{\sigma_{xy}^{o}}{\rho_c h} + \dfrac{2 s_r \rho_{sy}}{\phi_y \rho_c \cos\theta_r} \displaystyle\int_{|\xi|}^{1} \tau_y(s) ds + g_n + \tan\theta_r \, g_t \\ \dfrac{1}{\rho_c} \sigma_{xy}^{o} \end{pmatrix} \tag{18}$$

$$\boldsymbol{\sigma}^{sx}(\xi) = \left[\frac{1}{\rho_{sx} h} \left(\sigma_{xx}^{o} - \frac{\sigma_{xy}^{o}}{\tan\theta_r} \right) + \frac{2 s_r}{\phi_x \sin\theta_r} \int_{|\xi|}^{1} \tau_x(s) ds - \frac{\rho_c}{\rho_{sx}} \left(g_n - \frac{1}{\tan\theta_r} g_t \right) \right] \cdot \underline{e}_x \otimes \underline{e}_x \tag{19}$$

$$\boldsymbol{\sigma}^{sy}(\xi) = \left[\frac{1}{\rho_{sy} h} \left(\sigma_{yy}^{o} - \sigma_{xy}^{o} \tan\theta_r \right) - \frac{2 s_r}{\phi_y \cos\theta_r} \int_{|\xi|}^{1} \tau_y(s) ds - \frac{\rho_c}{\rho_{sy}} \left(g_n + \tan\theta_r \, g_t \right) \right] \cdot \underline{e}_y \otimes \underline{e}_y \tag{20}$$

4.3 Local strain fields

The concrete and steel reinforcement local strain fields are obtained by applying the constitutive models (1) and (2) to the obtained local stress fields of the previous section:

$$\begin{pmatrix} \varepsilon_{xx}^{c}(\xi) \\ \varepsilon_{yy}^{c}(\xi) \\ \varepsilon_{xy}^{c}(\xi) \end{pmatrix} = \begin{pmatrix} \dfrac{\sigma_{xy}^{o}}{E_c \rho_c h} \left(\dfrac{1}{\tan\theta_r} - \nu_c \tan\theta_r \right) - \dfrac{2 s_r}{E_c \rho_c} \displaystyle\int_{|\xi|}^{1} \left(\dfrac{\rho_x \tau_x(s)}{\phi_x \sin\theta_r} + \dfrac{\nu_c \rho_y \tau_y(s)}{\phi_y \cos\theta_r} \right) ds + \dfrac{g_n}{E_c}(1 - \nu_c) - \dfrac{g_t}{E_c} \left(\dfrac{1}{\tan\theta_r} + \nu_c \tan\theta \right) \\ \dfrac{\sigma_{xy}^{o}}{E_c \rho_c h} \left(\tan\theta_r - \dfrac{\nu_c}{\tan\theta_r} \right) + \dfrac{2 s_r}{E_c \rho_c} \displaystyle\int_{|\xi|}^{1} \left(\dfrac{\nu_c \rho_{sx} \tau_x(s)}{\phi_x \sin\theta_r} + \dfrac{\rho_{sy} \tau_y(s)}{\phi_y \cos\theta_r} \right) ds + \dfrac{g_n}{E_c}(1 - \nu_c) + \dfrac{g_t}{E_c} \left(\tan\theta_r + \dfrac{\nu_c}{\tan\theta_r} \right) \\ \dfrac{1 + \nu_c}{E_c \rho_c h} \sigma_{xy}^{o} \end{pmatrix} \tag{21}$$

$$\varepsilon_{xx}^{sx}(\xi) = \frac{1}{E_{sx} \rho_{sx} h} \left(\sigma_{xx}^{o} - \frac{\sigma_{xy}^{o}}{\tan\theta_r} \right) + \frac{2 s_r}{E_{sx} \phi_x \sin\theta_r} \int_{|\xi|}^{1} \tau_x(s) ds - \frac{\rho_c}{E_{sx} \rho_{sx}} \left(g_n - \frac{1}{\tan\theta_r} g_t \right) \tag{22}$$

$$\varepsilon_{yy}^{sy}(\xi) = \frac{1}{E_{sy} \rho_{sy} h} \left(\sigma_{yy}^{o} - \sigma_{xy}^{o} \tan\theta_r \right) - \frac{2 s_r}{E_{sy} \phi_y \cos\theta_r} \int_{|\xi|}^{1} \tau_y(s) ds - \frac{\rho_c}{E_{sy} \rho_{sy}} \left(g_n + \tan\theta_r \, g_t \right) \tag{23}$$

4.4 Compatibility of strains

For a medium with no displacement discontinuities in the RVE, the membrane generalized strain tensor $\boldsymbol{\varepsilon}^{\boldsymbol{o}}$ is given for any displacement field $\underline{u}$ by the direct application of (6):

$$\boldsymbol{\varepsilon}^{o} = \langle \boldsymbol{\varepsilon}(\underline{u}) \rangle_{\Omega} = \frac{1}{|\Omega|} \int_{\Omega} \boldsymbol{\varepsilon}(\underline{u}) \, dv \tag{24}$$

When a displacement discontinuity $[\![\underline{u}]\!]$ on a particular regular boundary Γ within the RVE is considered (denoting by $\underline{n}$ the local unit normal vector on Γ and by $\otimes^s$ the symmetric dyadic tensor product), the following amendment of the previous expression is made (referring to the Stokes' theorem):

$$\boldsymbol{\varepsilon}^o = \frac{1}{|\Omega|}\left(\int_{\Omega} \boldsymbol{\varepsilon}(\underline{u})\, dv + \int_{\Gamma} [\![\underline{u}]\!] \otimes^s \underline{n}\, dv\right) \tag{25}$$

Equation (24) is used for the calculation of ε_{xx}^o and ε_{yy}^o from x and y steel bars strain fields respectively, while (25) is used for calculating the three components of $\boldsymbol{\varepsilon}^o$ from the concrete local strain field, with $[\![\underline{u}]\!]$ the displacement discontinuity at cracks $\underline{w}$:

$$\begin{cases} \varepsilon_{xx}^o = \langle \varepsilon_{xx}^{sx} \rangle \\ \varepsilon_{yy}^o = \langle \varepsilon_{yy}^{sy} \rangle \\ \boldsymbol{\varepsilon}^o = \langle \boldsymbol{\varepsilon}^c \rangle + \dfrac{1}{s_r} \underline{w} \otimes^s \underline{n} \end{cases} \tag{26}$$

where the equivalent strains due to cracks in the $x - y$ coordinates system are calculated as:

$$\frac{1}{s_r} \underline{w} \otimes^s \underline{n} = \frac{1}{2s_r}\begin{pmatrix} 2w_n \sin^2\theta_r - w_t \sin 2\theta_r & -w_n \sin 2\theta_r + w_t \cos 2\theta_r \\ -w_n \sin 2\theta_r + w_t \cos 2\theta_r & 2w_n \cos^2\theta_r + w_t \sin 2\theta_r \end{pmatrix} \tag{27}$$

The averages of the local strain fields (21), (22) and (23) are calculated with (7) and inserted in (26). A five equations system linking the stress resultants $\boldsymbol{\sigma}^o$ to the generalized strains $\boldsymbol{\varepsilon}^o$ and the internal variables is obtained:

$$\begin{cases} \varepsilon_{xx}^o = \dfrac{1}{E_{sx}\rho_{sx}h}\left(\sigma_{xx}^o - \dfrac{\sigma_{xy}^o}{\tan\theta_r}\right) + \dfrac{2s_r\tau_x^o}{E_{sx}\phi_x \sin\theta_r} - \dfrac{\rho_c}{E_{sx}\rho_{sx}}\left(g_n - \dfrac{g_t}{\tan\theta_r}\right) \\ \varepsilon_{yy}^o = \dfrac{1}{E_{sy}\rho_{sy}h}\left(\sigma_{yy}^o - \sigma_{xy}^o \tan\theta_r\right) - \dfrac{2s_r\tau_y^o}{E_{sy}\phi_y \cos\theta_r} - \dfrac{\rho_c}{E_{sy}\rho_{sy}}\left(g_n + \tan\theta_r\, g_t\right) \\ \varepsilon_{xx}^o = \dfrac{\sigma_{xy}^o}{E_c\rho_c h}\left(\dfrac{1}{\tan\theta_r} - \nu_c \tan\theta_r\right) - \dfrac{2s_r}{E_c\rho_c}\left(\dfrac{\rho_{sx}\tau_x^o}{\phi_x \sin\theta_r} + \dfrac{\nu_c\rho_{sy}\tau_y^o}{\phi_y\cos\theta_r}\right) + \dfrac{g_n}{E_c}(1-\nu_c) - \dfrac{g_t}{E_c}\left(\dfrac{1}{\tan\theta_r} + \nu_c \tan\theta_r\right) + \dfrac{w_n}{s_r}\sin^2\theta_r - \dfrac{\sin 2\theta_r}{2}\dfrac{w_t}{s_r} \\ \varepsilon_{yy}^o = \dfrac{\sigma_{xy}^o}{E_c\rho_c h}\left(\tan\theta_r - \dfrac{\nu_c}{\tan\theta_r}\right) + \dfrac{2s_r}{E_c\rho_c}\left(\dfrac{\nu_c\rho_{sx}\tau_x^o}{\phi_x \sin\theta_r} + \dfrac{\rho_{sy}\tau_y^o}{\phi_y\cos\theta_r}\right) + \dfrac{g_n}{E_c}(1-\nu_c) + \dfrac{g_t}{E_c}\left(\tan\theta_r + \dfrac{\nu_c}{\tan\theta_r}\right) + \dfrac{w_n}{s_r}\cos^2\theta_r + \dfrac{\sin 2\theta_r}{2}\dfrac{w_t}{s_r} \\ \varepsilon_{xy}^o = \dfrac{1+\nu_c}{E_c\rho_c h}\sigma_{xy}^o - \dfrac{\sin 2\theta_r}{2}\dfrac{w_n}{s_r} + \dfrac{\cos 2\theta_r}{2}\dfrac{w_t}{s_r} \end{cases} \tag{28}$$

where the average bond-slip stress is defined:

$$\tau_\alpha^o = \langle \int_{|\xi|}^{1} \tau_\alpha(z)dz \rangle = \int_0^1 \int_{|\xi|}^{1} \tau_\alpha(z)dz\, d\xi \quad \alpha = x, y \tag{29}$$

Details about these developments and the complete thermodynamic formulation of the general model can be found in [13]. We briefly describe hereafter a particular one-dimensional case.

5 EXAMPLE: A ONE-DIMENSIONAL DAMAGE MODEL

As an example of application of the developed general model, one of the simplest particular cases is reproduced hereafter: a one-dimensional damage model where crack development and bond stresses are not explicitly taken into account. The GLRC_DM [2] damage approach accounting for a constant slope in the $\boldsymbol{\sigma}^o - \boldsymbol{\varepsilon}^o$ relationship while damage evolves is adopted.

First, we solve the equations system (28) for a member reinforced only in the x direction ($\rho_{sy} = 0$) submitted to σ^o_{xx} stress ($\sigma^o_{yy} = \sigma^o_{xy} = 0$). Considering no distortion ($\varepsilon^o_{xy} = 0$) and that cracks appear orthogonally to the x direction ($\theta_r = \frac{\pi}{2}$), the following $\sigma^o_{xx} - \varepsilon^o_{xx}$ relationship can be obtained:

$$\sigma^o_{xx} = h \cdot \left(\rho_{sx} E_{sx} \varepsilon^o_{xx} + \rho_c g_n - \frac{2\tau^0_x \rho_{sx} s_r}{\phi_x} \right) \tag{30}$$

The expression for the crack opening is also obtained:

$$w_n = s_r \cdot \left(\varepsilon^o_{xx} - \frac{g_n}{E_c} + \frac{2\rho_{sx} s_r \tau^o_x}{\rho_c \phi_x E_c} \right) \tag{31}$$

In a damage model where no crack opening is taken into account, bond stress between concrete and steel vanishes, and thus w_n and τ^o_x are set to zero in (31), obtaining the following value for stress g_n:

$$g_n = \varepsilon^o_{xx} E_c \tag{32}$$

Using the previous condition and adding the dependency of the concrete Young modulus with the scalar damage variable d, constitutive relationship (30) reads:

$$\sigma^o_{xx} = h \cdot \left(\rho_{sx} E_{sx} + \rho_c E_c(d) \right) \varepsilon^o_{xx} \tag{33}$$

The adopted free energy density is:

$$\varphi(\varepsilon^o_{xx}, d) = \frac{h}{2} \left(\rho_{sx} E_{sx} + \rho_c E_c(d) \right) (\varepsilon^o_{xx})^2 \tag{34}$$

The energy release rate reads (assuming $E'_c(d) \leq 0$ and $E''_c(d) > 0$):

$$Y = -\frac{\partial \varphi}{\partial d} = -\frac{h}{2} \rho_c E'_c(d) (\varepsilon^o_{xx})^2 \tag{35}$$

The yield function is (assuming no hardening):

$$f(Y) = |Y| - k_0 \leq 0 \tag{36}$$

Then the tangent slope $E^o(d)$ is deduced:

$$E^o(d) = \frac{d\sigma^o_{xx}}{d\varepsilon^o_{xx}} = h \cdot \left(\rho_{sx} E_{sx} + \rho_c E_c(d) \right) + h \rho_c E'_c(d) \frac{\partial d}{\partial \varepsilon^o_{xx}} \varepsilon^o_{xx} \tag{37}$$

In the damage evolution phase, $\frac{\partial d}{\partial \varepsilon^o_{xx}}$ is obtained with the $\dot{f} = 0$ consistency condition:

$$\dot{f} = 0 \Rightarrow 2E'_c(d) \varepsilon^o_{xx} + E''_c(d) \frac{\partial d}{\partial \varepsilon^o_{xx}} (\varepsilon^o_{xx})^2 = 0 \Rightarrow \frac{\partial d}{\partial \varepsilon^o_{xx}} = -\frac{2E'_c(d)}{E''_c(d) \varepsilon^o_{xx}} \tag{38}$$

And finally the slope of the strain-stress resultant curve reads:

$$E^o(d) = \frac{d\sigma^o_{xx}}{d\varepsilon^o_{xx}} = h \rho_{sx} E_{sx} + h \rho_c \left(E_c(d) - \frac{2\left(E'_c(d)\right)^2}{E''_c(d)} \right) \tag{39}$$

The slope in the damage evolution phase in GLRC_DM model is constant and it is noted as $E^{o,c}$ for compression loadings and $E^{o,t}$ for tension ones. Thus, from (39), the $E_c(d)$ function has the form:

$$E_c(d) = H(\varepsilon_{xx}^o)E_{c,o}\frac{a_c + \dfrac{E^{o,t} - \dfrac{\rho_{sx}}{\rho_c}E_{sx}}{E_{c,o}}d}{a_c + d}(\varepsilon_{xx}^o) + H(-\varepsilon_{xx}^o)E_{c,o}\frac{a_t + \dfrac{E^{o,c} - \dfrac{\rho_{sx}}{\rho_c}E_{sx}}{E_{c,o}}d}{a_t + d} \tag{40}$$

with a_c, a_t undefined parameters.

This model is applied to the experimental test described in [14], consisting in a one-dimensional RC member $0.7m$ length, $150\text{x}150mm^2$ section, reinforced with 4 rebars ($\phi_x = 14mm$ diameter) and Young modulus $E_{sx} = 195GPa$, and with a concrete characterized by an initial Young modulus $E_{c,o} = 28.5GPa$, tensile strength $f_{ct} = 2.94MPa$ and compressive strength $f_c = 50MPa$. $E^{o,c}$ and $E^{o,t}$ parameters are set to $-0.03E_{c,o}$ and $0.3E_{c,o}$ respectively, and a_t is set to 1. Finally, we use $k_0 = 117N/m$ and $a_c = 9.4$ in order to set the damage beginning at f_{ct} for tension loadings and $f_c/2$ for the compression ones.

The comparison of Figure 4 (a) between the experimental and the numerical results shows a quite good agreement. However, dissipation is underestimated as long as the hysteretic experimental response is not well reproduced. In [13] it is showed that the dissipation can be better assessed for the tension loading domain when the developed model in section 4 is applied for the case where crack opening is allowed and modeled using suitable functions for bond stresses and concrete stress transfer at cracks; the obtained results with this model are also plotted in Figure 4 (b).

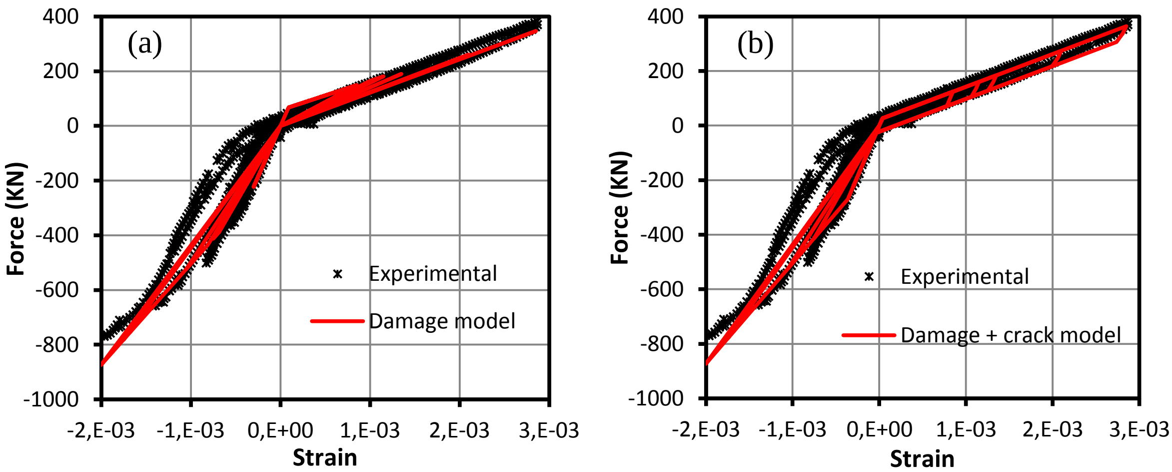

Figure 4: Comparison between numerical and experiment results for a one-dimensional RC member

6 CONCLUSIONS

A general nonlinear constitutive model for RC panels has been developed. Nonlinear phenomena at the local scale (concrete micro and macro cracking, steel-concrete debonding) appear in an explicit manner by means of general functions on the global formulation of the model as a result of an analytical homogenization technique. A particular one-dimensional case is finally presented in order to show the applicability of the model.

ACKNOWLEGDEMENTS

This work, performed within the RSRN project ("Recherche dans le domaine de la Sureté Nucléaire et de la Radioprotection"), has been financed by the French Agence Nationale de la Recherche, program "Investissements d'avenir", ANR-11-RSNR-0022 (ANR SINAPS@), and the first author is also partly supported by the French Association Nationale de la Recherche et de la Technologie.

REFERENCES

[1] Code_Aster, general public licensed structural mechanics finite element software, Internet site: http://www.code-aster.org

[2] Markovic, D., Koechlin, P. and Voldoire, F., Reinforced concrete structures under extreme loading: Stress resultant Global Reinforced Concrete Models (GLRC). *Proc. COMPDYN 2007*, Rethymno, Greece.

[3] Combescure, C., Dumontet, H. and Voldoire, F. Homogenized constitutive model coupling damage and debonding for reinforced concrete structures under cyclic solicitations. *Int. J. Solids Struct.* (2013) **50**:3861-3874.

[4] Halphen, B. and Nguyen, Q.S. Sur les matériaux standards généralisés. *J. Mécanique* (1975) **14**:39-63.

[5] Lemaitre, J. and Chaboche, J.L. *Mechanics of Solid Materials*. Cambridge University Press (1994).

[6] Ruocci, G., Huguet, M., Erlicher, S. and Bisch, P. Crack orientation, distance and width in reinforced concrete membranes: experimental results and preliminary interpretations based on the Cracked Membrane Model. *Proc. TINCE 2013*, Paris, France.

[7] Kaufmann, W. and Marti, P. Structural concrete: cracked membrane model. *J. Struct. Eng.* (1998) **124**(12):1467-1475.

[8] Vecchio, F.J. and Collins, M.P. The modified compression field theory for reinforced concrete elements subjected to shear. *ACI Journal* (1986) **83**(2):219-231.

[9] Pimentel, M., Bruwhiler, E. and Figueiras, J. Extended cracked membrane model for the analysis of RC panels. *Eng. Struct.* (2010) **32**:1964-1975.

[10] Palermo, D. and Vecchio, F.J. Compression field modeling of reinforced concrete subjected to reversed loading: formulation. *ACI Struct. J.* (2003) **100**(5):616-625.

[11] Fédération Internationale du Béton (*fib*). *Model Code 2010*.

[12] Sanchez-Palencia, E., Zaoui, A. and Suquet, P. *Homogenization Technique for Composite Media*. Springer, Berlin Heidelberg (1987).

[13] Huguet, M., Erlicher, S., Kotronis, P. and Voldoire, F. Homogenized nonlinear stress resultant constitutive model for cracked reinforced concrete panels. *Int. J. Solids Struct.* (under submission).

[14] Benmansour, M.B. *Modélisation du comportement cyclique alterné du béton armé. Application à divers essais statiques de poteaux.* PhD Thesis, Ecole Nationale des Ponts et Chaussées (1997).